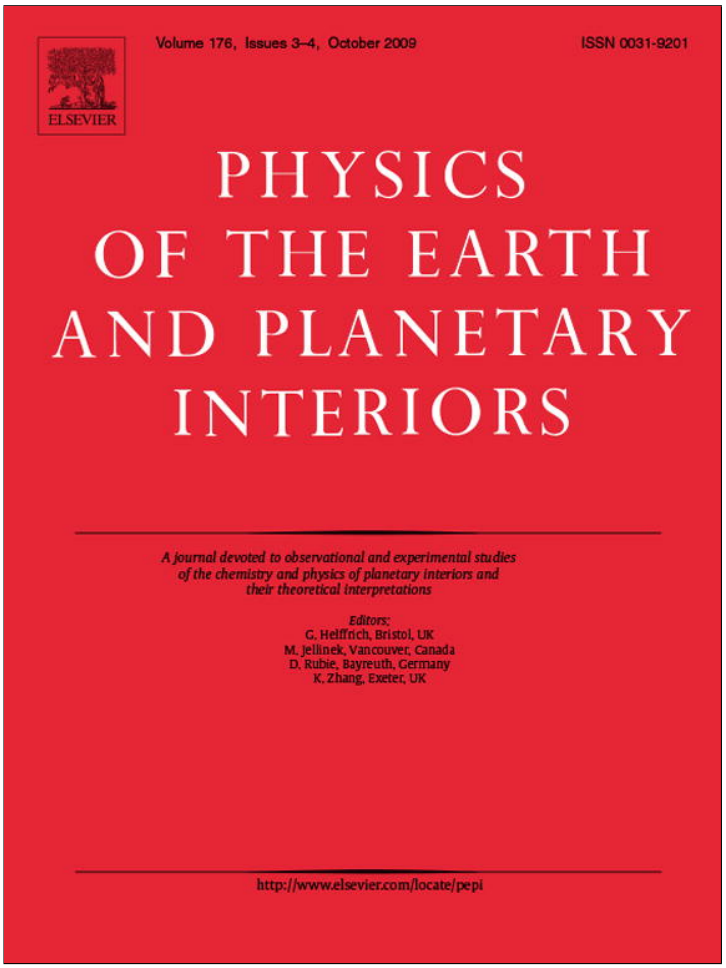

Physics of the Earth and Planetary Interiors 176 (2009) 187–197

Contents lists available at ScienceDirect

Physics of the Earth and Planetary Interiors

journal homepage: www.elsevier.com/locate/pepi

The relative wavelengths of fast and slow velocity anomalies in the lower mantle: Contrary to the expectations of dynamics?

Christine Houser*, Quentin Williams

Department of Earth and Planetary Sciences, University of California Santa Cruz, 1156 High Street, Santa Cruz, CA 95064, United States

ARTICLE INFO

Article history:
Received 19 January 2008
Received in revised form 1 May 2009
Accepted 1 May 2009

Keywords:
Tomography
Mantle structure
Mantle convection

ABSTRACT

We quantify the spherical harmonic characteristics of shear velocity anomalies as a function of depth for a range of tomographic models of the Earth's mantle. In particular, the amplitude spectra of fast and slow anomalies are analyzed separately. Thus, the higher amplitude harmonic degrees and relative scale lengths of both possible thermal upwellings and downwellings can be determined. Our results are consistent with prior studies in that we find that the amplitude spectra of heterogeneity (fast and slow) in the mid-mantle are essentially flat. However, where heterogeneity is known to be stronger in the deep mantle, slow anomalies are observed to be consistently higher amplitude at harmonic degrees 1–12, while fast anomalies dominate at higher degrees. This result is at odds with many dynamic models in which upwellings tend to be narrow and downwellings tend to be broad. This inconsistency with isochemical dynamic models may be associated with variations in phase, chemistry and/or viscosity in the Earth's lowermost mantle. The technique presented here provides a means for discriminating between these effects when comparing tomographic and dynamic models of the Earth's mantle.

From a parsimonious observational viewpoint, we know cold oceanic lithosphere is subducting into the interior of our planet, and we observe hot spots at the surface that may be a consequence of heat transfer from the core to the mantle (Sleep, 1990; Courtillot et al., 2003). Since its beginnings, seismic tomography has been viewed as reflecting the pattern of mantle dynamics (Dziewonski et al., 1977; Hager et al., 1985), although tomographic velocity heterogeneities likely reflect both thermal and compositional effects, which are difficult to distinguish from one another. Recent seismic tomographic models with ever-increasing resolution can, in principle, constrain progressively finer details of mantle dynamics. Here, we evaluate velocity anomaly patterns in terms of our current understanding of the planform of mantle convection, with the expectation that the scale lengths of upwellings and downwellings might best be observed in the latest generation of tomographic models. Both laboratory and computational models of simple mantle circulation (which include heating from below, cooling from above and variable amounts of internal heating) uniformly indicate that the mantle should be characterized by narrow upwellings and broad, possibly sheet-like downwellings (Tackley et al., 1993; Zhang and Yuen, 1996; Bunge et al., 1997; Zhong and Gurnis, 1997; Tan and Gurnis, 2002; Nakagawa and Tackley, 2004; McNamara and Zhong, 2005). In detail, the depth dependence of the widths of these features may relate to the degree of internal heating relative to heating from below (Bunge, 2005). However, we demonstrate and quantify that the opposite pattern is observed in the deep mantle: the base of the mantle appears to be dominated by broad slow anomalies (upwellings?) and narrow fast anomalies (downwellings?).

For this analysis, we use a suite of recent mantle shear velocity models based on long-period seismic data; HMSL-S06 (Houser et al., 2008), TX2006 (Simmons et al., 2006), PRI-S05 (Montelli et al., 2006), J362D28 (Antolik et al., 2003), S20RTS (Ritsema and van Heijst, 2000), and SAW24B16 (Megnin and Romanowicz, 2000). These models are derived using a variety of datasets, parameterizations, inversion techniques, and regularizations, with the details of their derivation summarized elsewhere (Hernlund and Houser, 2008). We analyze all six of these models, but focus particularly on model HMSL-S06, which is parameterized as 18 layers of 100 km thickness in the upper mantle and 200 km thickness in the lower mantle divided into equal area blocks measuring 4° at the equator. Numerous phases are compiled to provide continuous coverage of the upper to lower mantle. Love and Rayleigh phase velocity maps (Bassin et al., 2000) are used to constrain the upper mantle. Differential *SS-S* and *ScS-S* data (Woodward and Masters, 1991a, 1991b) are updated with events through 1999 and 2005, respectively, to improve body wave coverage of the mid- and lowermost mantle. The bulk of the data are *S* and *SS* arrival times compiled through 2005 using the cluster analysis method of Houser et al. (2008). HMSL-S06 is thus a robust model with extensive coverage of the mid

* Corresponding author.
E-mail address: cthouser@ucsc.edu (C. Houser).

0031-9201/$ – see front matter © 2009 Elsevier B.V. All rights reserved.
doi:10.1016/j.pepi.2009.05.001

and deep mantle, making it ideal for studying connections between upper- and lower-mantle structures.

For decades, tomography has resolved very slow and very fast features at the core-mantle boundary (CMB). It has been postulated that these fast anomalies at the CMB are due to the accumulation of slab material (van der Hilst et al., 1997). Kellogg et al. (1999) proposed a model in which slabs may be inhibited by a chemical layer before reaching the CMB, but there is no tomographic evidence for slab accumulation in the mid or lower mantle. Regions of very slow anomalies above the CMB under Africa and the central Pacific are expressed, in spherical harmonic representation, by a dominance in degree 2 at these depths (Su and Dziewonski, 1991). These slow regions are likely associated with surface hot spots (Thorne et al., 2004), but the precise physical connection has been difficult to prove. The African and Pacific large low shear velocity provinces (LLSVP) have been proposed to act as "plume farms," (Schubert et al., 2004) with narrow plumes being derived from their tops. If plumes do rise off of the tops of these features, tomography may not resolve these finer-scale structures, and consequently the amplitude of the characteristic degree 2 signature would diminish. The overall morphology of the models demonstrates that the relationship between the fast and slow anomalies at the CMB and those in the overlying mantle requires further investigation.

Most dynamic models of a chemically homogeneous mantle indicate that cold, downwelling oceanic lithosphere is expected to grossly maintain its integrity as a tabular or cylindrical, cold anomaly from the surface to the CMB. Similarly, upwelling plumes are likely to be narrow cylindrical features extending from the CMB to the surface (Tackley et al., 1993; Zhang and Yuen, 1996; Bunge et al., 1997; Tan and Gurnis, 2002). Furthermore, fluid dynamic simulations and calculations indicate that broadened roots of hot spots may be present near the CMB (Davaille et al., 2003; Jellinek and Manga, 2004). If these calculations and simulations accurately represent the Earth's mantle, then at least the broadest portions of these patterns should be resolvable with seismic tomography. While it is difficult to trace a particular slab or plume between CMB depths and the surface, it is possible to observe changes in the horizontal scale length of fast and slow anomalies with depth. That is, we can determine whether the amplitudes of positive and negative velocity heterogeneities are concentrated in low order (long wavelength) or high order (short wavelength) spherical harmonics and observe how this pattern changes with depth. We expect that slabs ponding at the CMB should result in fast anomalies with high amplitudes in the low order spherical harmonics. The LLSVP signature should cause amplitudes to be dominant at degree 2 in the lowermost mantle and possibly transition to higher order spherical harmonics in the mid- to upper mantle.

To test these expectations, we divide the tomographic models into two portions, one containing only the fast anomalies and the other only the slow anomalies. In each case, the remaining portion of the model is set to zero. We define fast or slow anomalies by removing the mean velocity at each depth. Thus, we examine the size, shape and amplitude of the respective positive and negative velocity anomalies. It is this separation of the heterogeneity field into fast and slow components that distinguishes our approach from a number of previous global inversions for the depth dependence of power spectra in both tomographic and fluid dynamic models. Typically, the fast and slow anomalies have not been separated in determining such power spectra (Woodward et al., 1994; Bunge et al., 1996; Megnin et al., 1997; Gu et al., 2001; Deschamps and Tackley, 2008), or the skewness of the entire velocity structure has been probed (Yanagisawa and Hamano, 1999). Becker and Boschi (2002) separated fast and slow anomalies at two depths (550 and 850 km) to test whether correlations between tomographic models and cold and hot features in dynamic models were improved by the separation. Recently, Boschi et al. (2007) use our

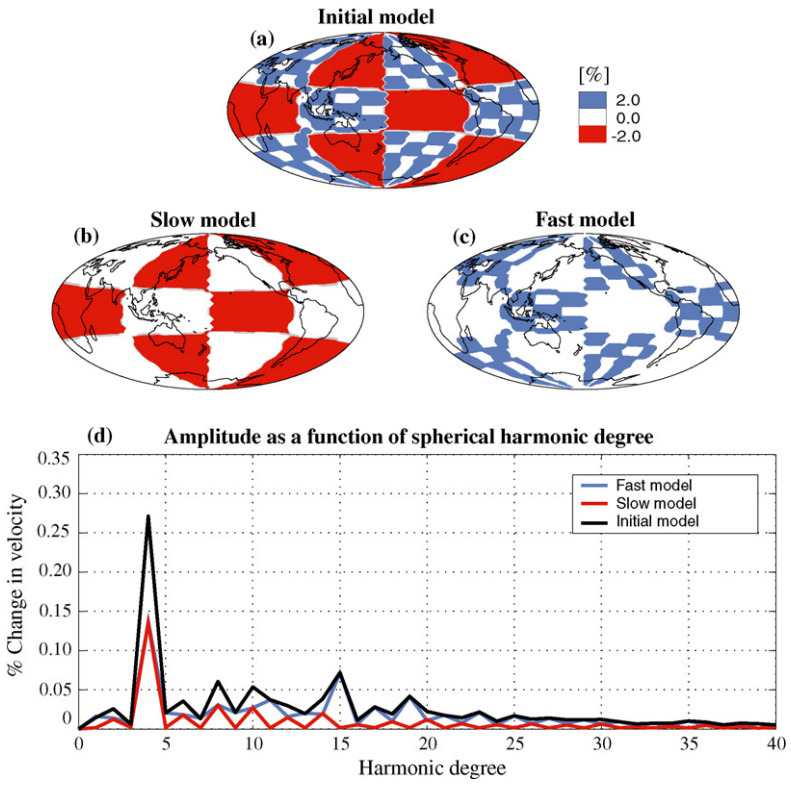

Fig. 1. An initial checkerboard model (a) is divided into a model with only slow (red) anomalies (b) and a model with only fast (blue) anomalies (c). The amplitude as a function of spherical harmonic degree is shown in part (d) for the initial model (thick black line), the fast model (blue line), and the slow model (red line). (For interpretation of the references to colour in this figure legend, the reader is referred to the web version of the article.)

separation technique presented here (with our permission) in their evaluation of tomographic models. Their work provides analysis of the correlations of the recent tomographic models with dynamic models using different assumptions for upwelling plumes. However, here we present the first amplitude spectra analysis of the lower mantle for the latest generation of long-period tomographic models as well as the average models SMEAN and PMEAN (Becker and Boschi, 2002) to assess the depth dependence of the wavelengths of structural features within the mantle.

The existence and depth dependence of asymmetry between the length-scales of upwellings and downwellings has not been quantitatively explored. Indeed, the strong amplitudes of the slow anomalies in the deep mantle typically dominate the spherical harmonic analyses of tomographic models, and thus our separation of the fast anomalies allows us to reveal their spatial scale independently from the slow anomalies. In addition, previous studies concentrated on determining the general agreement of the power spectra as a function of depth between tomographic and dynamic models, with the goal to evaluate layered versus whole-mantle convection. Here, we take advantage of the finer resolution of the most recent tomographic models coupled with the separate treatment of fast and slow anomalies to further constrain the characteristics of mantle convection.

A sample test-case for our approach, an application to a checkerboard model, is shown in Fig. 1. The initial model (Fig. 1a) is divided into two portions, a model with only slow anomalies (Fig. 1b) and a model with only fast anomalies (Fig. 1c). The amplitude as a function of spherical harmonic degree is shown in Fig. 1d for the initial model (black), the fast model (blue), and the slow model (red). The complex spherical harmonic coefficients ($a = real$, $b = imaginary$) are fully normalized as defined by Edmonds (1960). The power and amplitude spectrum are defined as follows:

$$\text{power} = \frac{\sum_{m=1}^{l} a^2 + b^2}{4\pi(2l+1)}$$

$$\text{amplitude} = \sqrt{\text{power}}$$

We evaluate the amplitude spectrum as opposed to the power spectrum since the amplitudes of the separated components of the

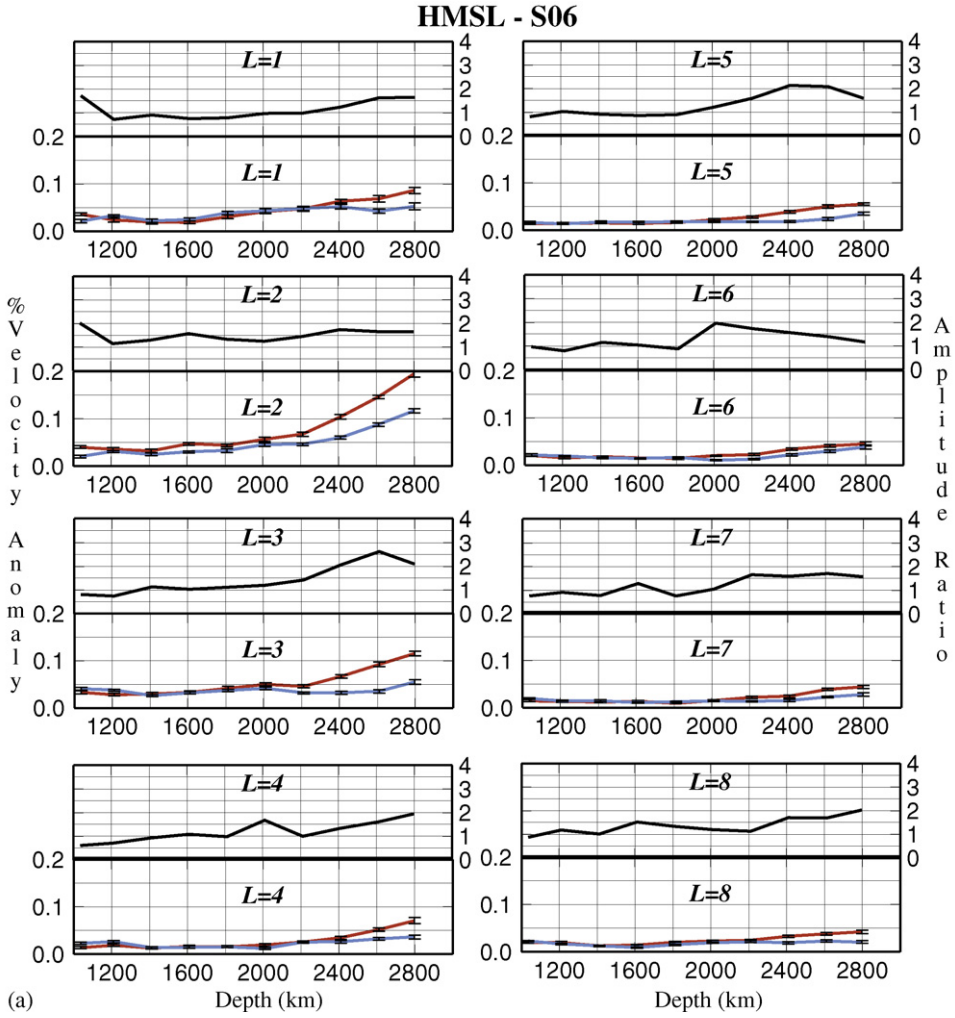

Fig. 2. Amplitude as a function of depth for spherical harmonic degrees 1–8 for the fast anomalies (blue) and slow anomalies (red) for the lower mantle of the shear velocity models (a) HMSL-S06 (Houser et al., 2008); (b) TX2006 (Simmons et al., 2006); (c) PRI-S05 (Montelli et al., 2006); (d) J362D28 (Antolik et al., 2003); (e) S20RTS (Ritsema and van Heijst, 2000); (f) SAW24B16 (Megnin and Romanowicz, 2000); and (g) SMEAN (Becker and Boschi, 2002). The black line in the top graph for each harmonic degree is the ratio of amplitudes of the slow and fast anomalies. This value is usually greater than one since the amplitudes of the slow anomalies are typically higher than the fast anomalies at most depths. The highest amplitude is observed in degree 2 for both the fast and slow anomalies in all the models. The amplitude in the slow anomalies is consistently higher than in the fast anomalies. Error bars are provided for model HMSL-S06 based on a Monte Carlo error analysis (Houser et al., 2008) in which Gaussian distributed noise is added to the data and the inversion is re-run 100 times, producing 100 different models. The error bars are the standard deviation on the spherical harmonic amplitudes calculated for the resulting 100 models. Note that these error bars are very small and indicate the robustness of this technique. (For interpretation of the references to colour in this figure legend, the reader is referred to the web version of the article.)

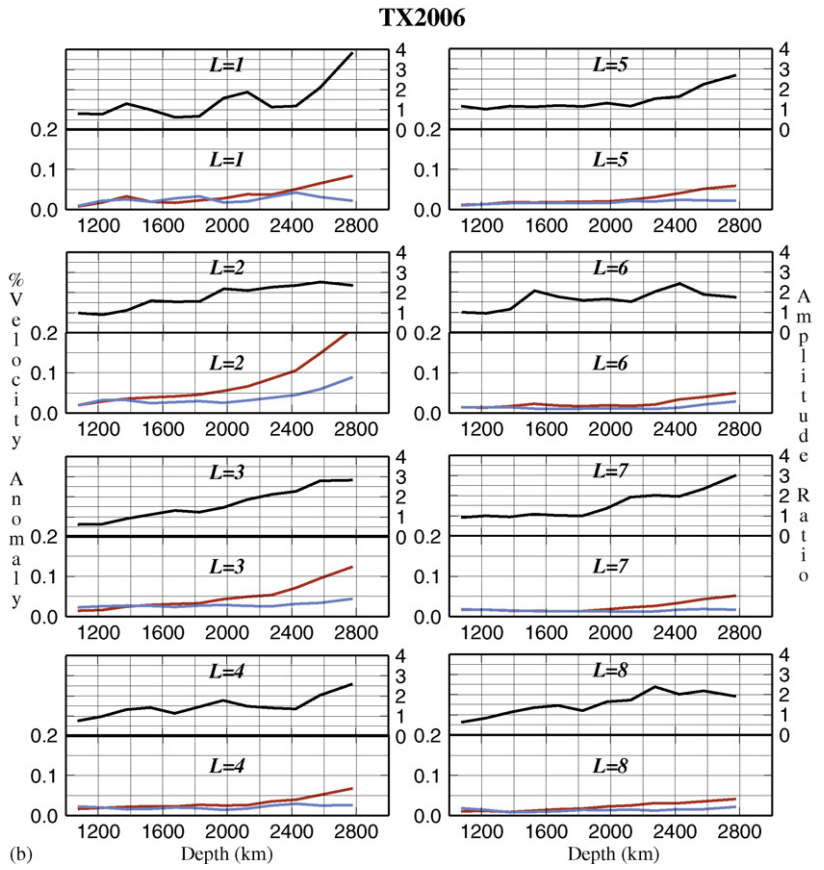

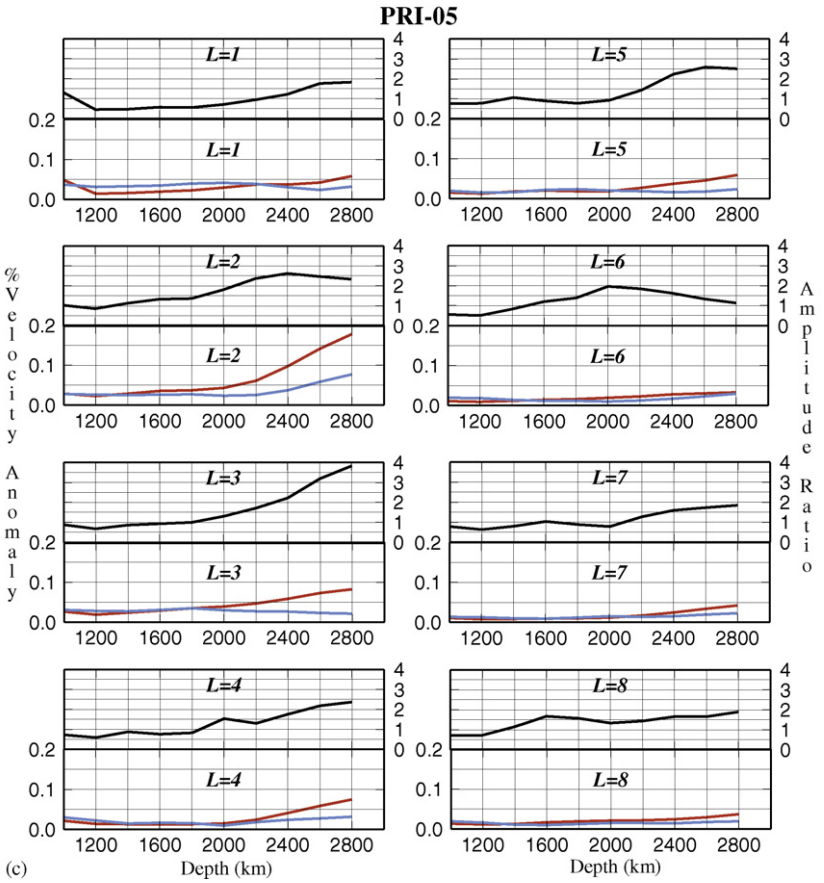

Fig. 2. (*Continued*)

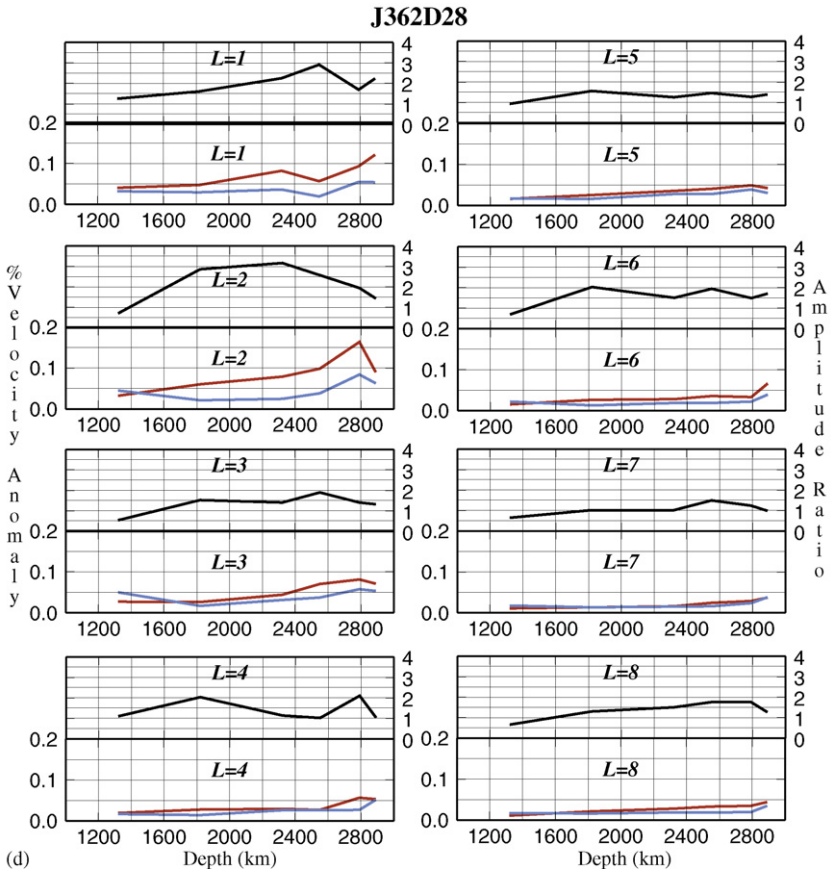

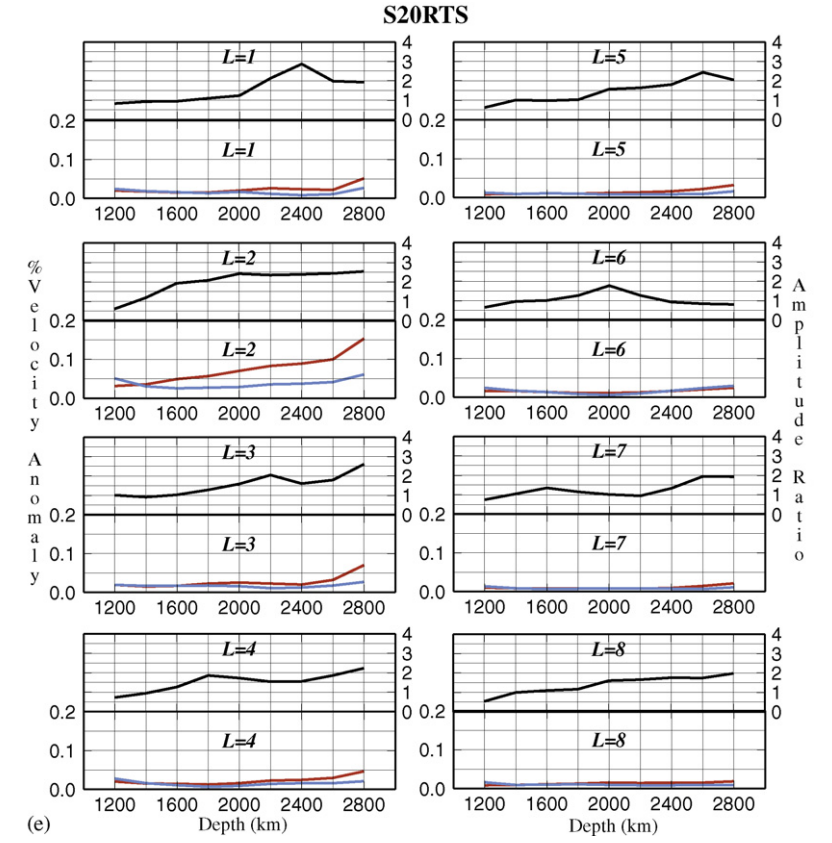

Fig. 2. (*Continued*)

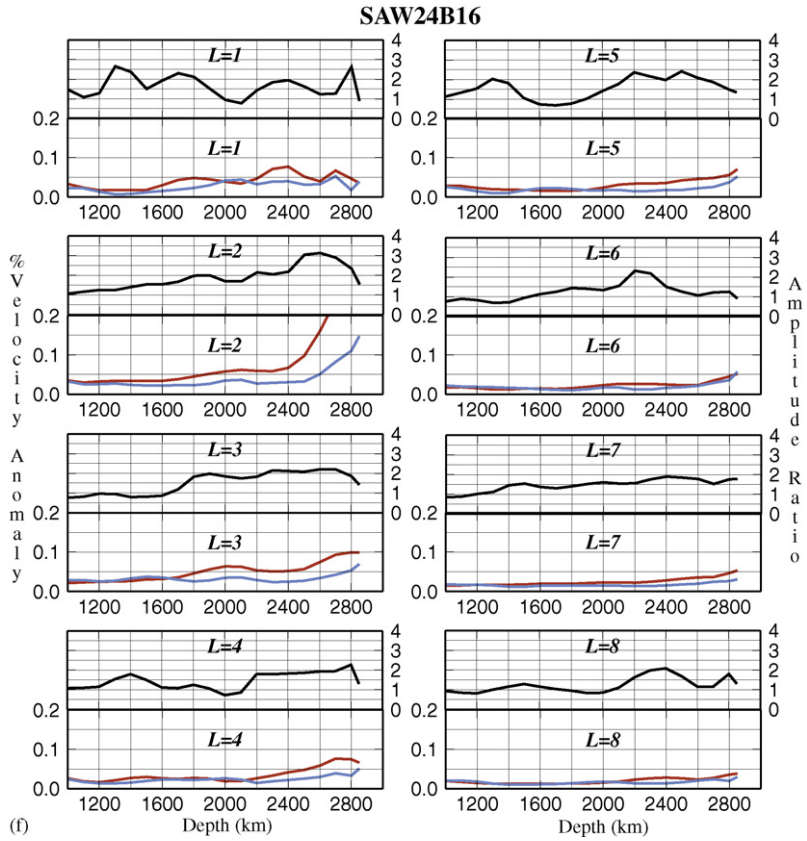

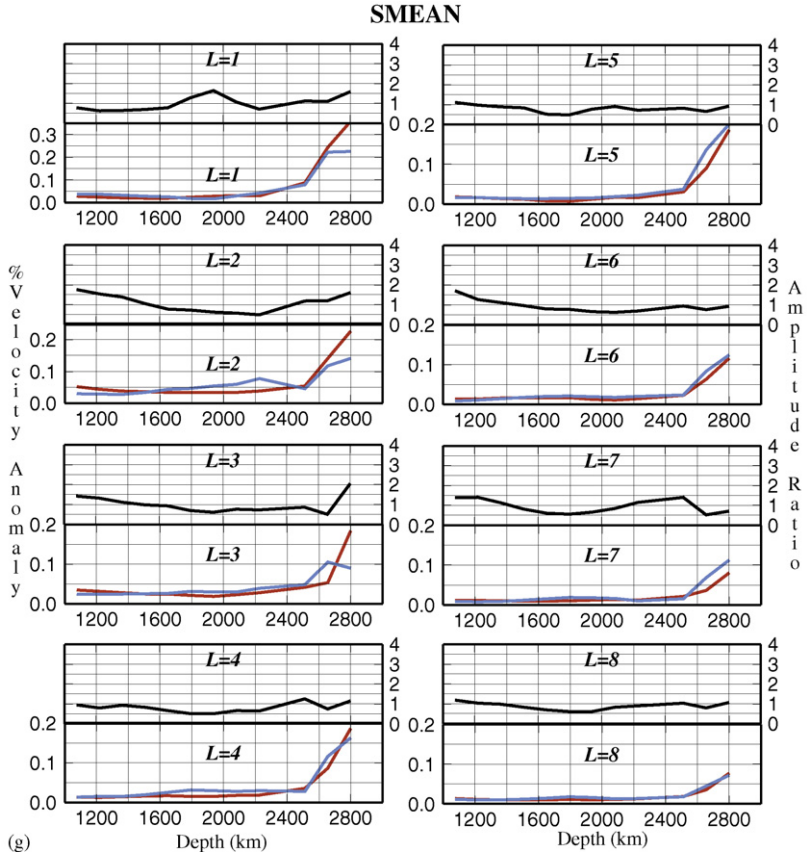

Fig. 2. (*Continued*).

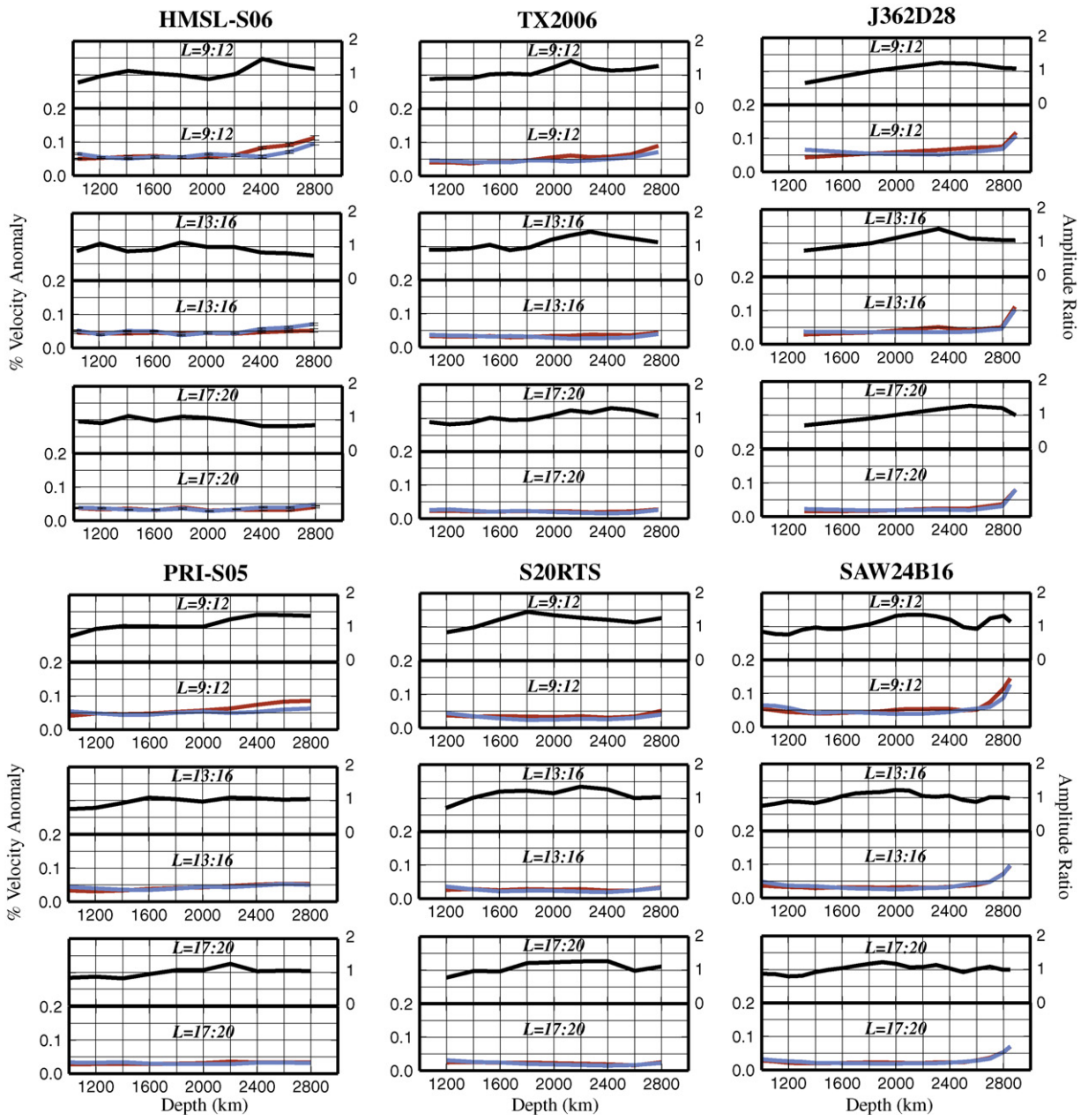

Fig. 3. Amplitude as a function of depth for the summation of spherical harmonic degrees 9–12 (top), 13–16 (middle), and 17–20 (bottom) for the fast anomalies (blue) and slow anomalies (red) for the lower mantle of the shear velocity models HMSL-S06 (Houser et al., 2008), TX2006 (Simmons et al., 2006), PRI-S05 (Montelli et al., 2006), J362D28 (Antolik et al., 2003), S20RTS (Ritsema and van Heijst, 2000), and SAW24B16 (Megnin and Romanowicz, 2000). The black line in the top graph for each harmonic degree is the ratio of amplitudes of the slow and fast anomalies. This value approaches one in the lower mantle since the amplitudes of the fast anomalies are equal to or greater than the slow anomalies at short wavelengths. The amplitude in the fast anomalies overcomes that in the slow anomalies as the harmonic degree increases (wavelength decreases) in model HMSL-S06 and acquires the same amplitude as the slow anomalies for the rest of the models. (For interpretation of the references to colour in this figure legend, the reader is referred to the web version of the article.)

velocity model add linearly. This is not the case for the power spectrum, since it is the square of the amplitude spectrum. Separating the model into fast and slow portions does introduce some ringing in the amplitude spectrum (Fig. 1d), but with amplitude that is well below the signal. The ringing occurs in both the positive and negative spectrum; therefore, a comparison of the two will be unbiased. In fact, the spectra in the individual fast or slow models do not contain any artifacts that are not present in the initial model. Thus, there is no information lost in the separation of the fast and slow spectra, only information gained in being able to evaluate the patterns of each individually without the signal of one being drowned out by the other. The fast and slow models both share a dominant degree 4 structure, but the fast model is further divided into a degree 15 structure which is apparent in Fig. 1d. Since the amplitude calculation is linear, the addition of the amplitude from the fast and slow models is equal to the total amplitude from the initial model. The spectrum of the positive and negative anomalies will be affected by the choice of the zero line that defines what is positive and what is negative. However, here we choose the zero line to agree with that used by the respective tomographic studies such that their associated amplitude spectra coincide with the published models. In addition, the character of the spectra does not change dramatically with small changes in the zero line. The layers of the models have different baseline shifts from the 1D models used to construct them, which are represented by the degree 0 term (Hernlund and Houser, 2008). These baseline shifts are often considered arbitrary and are

always removed when plotting and interpreting tomographic models. The precise origin of these baseline shifts is unclear, but here we are concerned with variations in lateral heterogeneity. The spectra of the lateral heterogeneity should be relatively insensitive to small shifts in model baselines at different depths.

The results of our analysis for a variety of tomographic models are shown in Fig. 2a–h as well as the average model SMEAN in Fig. 2g. We plot the changes in spherical harmonic amplitude with depth of the fast (blue) and slow (red) portions of the tomographic models for degrees 1 through 8. We also provide the ratio of the slow to fast amplitude as the black line in the top panel. For all of the models, the slow anomalies have larger or similar amplitude to the fast anomalies in the lowermost mantle. The amplitude in these low order harmonics then becomes very small around 1500 km depth. As a result, the spectrum of mantle heterogeneity is white in the mid-mantle, in accord with prior analyses of tomographic models (Woodward et al., 1994; Megnin et al., 1997; Gu et al., 2001). In Fig. 3, we show the summation of amplitude for degrees 9–12, 13–16, and 17–20 for the slow anomalies (red) and fast anomalies (blue). We bin these higher order harmonics simply because they have much less amplitude than the low order harmonics. For model HMSL-S06, the amplitude of the fast anomalies at harmonic degrees above 13 is larger than that of the slow anomalies in the lowermost 500 km of the mantle. This feature is not as pronounced in the other models in which the amplitude of the fast anomalies at large harmonic degrees approximately equals that of the slow anomalies in the deep mantle. Notably, this degree range is similar in spatial scale from that which might be associated with broadened slab-related features in the deep mantle. This is a resolved feature as indicated by the error bars. The error bars for model HMSL-S06 are the standard deviation on the harmonic amplitudes calculated for 100 different models constructed by adding Gaussian distributed noise to the data before each run of the inversion. The overarching observation is, however, that the slow anomalies have the largest amplitude in the lower mantle and are longer wavelength than the fast anomalies. This is contrary to the first-order dynamic inference that slow anomalies (upwellings) should be shorter wavelength than fast anomalies (downwellings).

Recent dynamic modelling (Tan and Gurnis, 2002; McNamara and Zhong, 2005) has attempted to explain the dominant degree 2 structure produced by the slow anomalies at the CMB with the suggestion that subducted slabs may effectively bulldoze slow and possibly chemically distinct material near the CMB into piles. In these models, the slabs are active features molding the basal layer into regional piles at the CMB, indicating that tomography ideally would detect (1) a continuous signature of slabs down to the CMB, and (2) a signal from positive velocity anomalies that is likely to be of similar amplitude as that of negative anomalies. The latter could be inaccurately represented in dynamic models of a homogeneous mantle, since velocity anomalies can arise not only from thermal anomalies, but also from chemical variations; and these thermal and chemical variations could either augment or offset

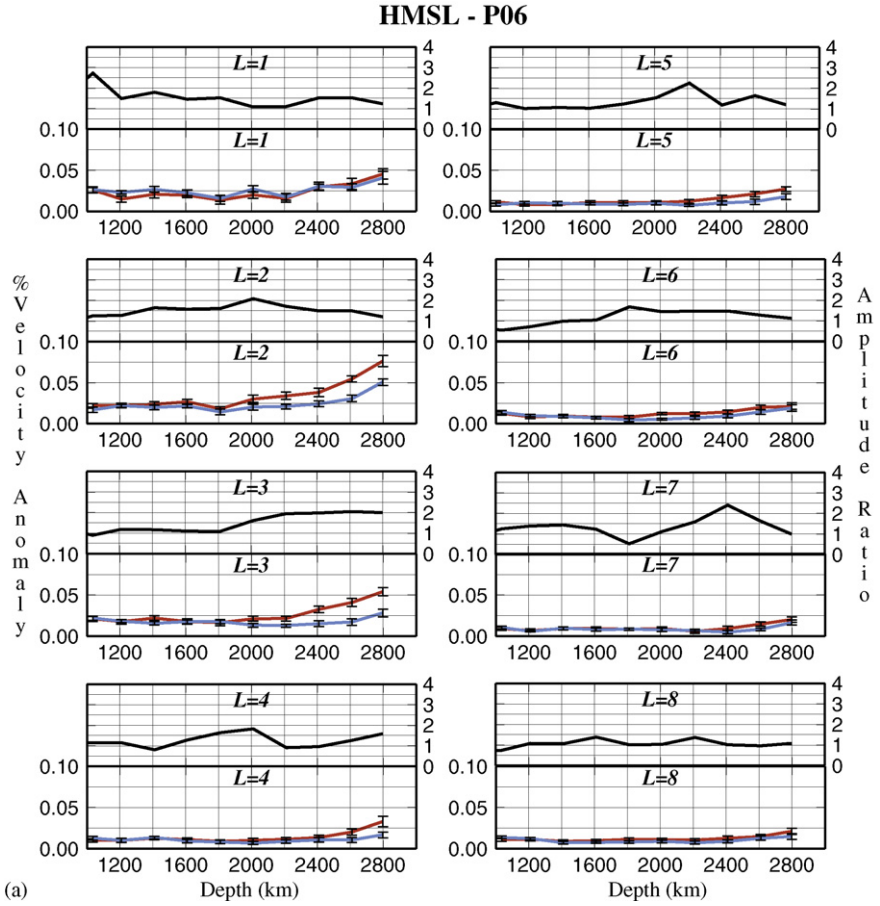

Fig. 4. Amplitude as a function of depth for spherical harmonic degrees 1–8 for the fast anomalies (blue) and slow anomalies (red) for the lower mantle of the compressional velocity model (a) HMSL-P06 (Houser et al., 2008) and (b) PMEAN (Becker and Boschi, 2002). The black line in the top graph for each harmonic degree is the ratio of amplitudes of the slow and fast anomalies. The highest amplitude is observed in degree 2 for both the fast and slow anomalies. Error bars are based on a Monte Carlo error analysis (Houser et al., 2008) in which Gaussian distributed noise is added to the data and the inversion is re-run 100 times, producing 100 different models. The error bars are the standard deviation on the spherical harmonic amplitudes calculated for the resulting 100 models. For HMSL-P06 the amplitude in the slow anomalies is consistently higher than in the fast anomalies. However, PMEAN has higher amplitude in the fast anomalies for degrees 1 and 3. (For interpretation of the references to colour in this figure legend, the reader is referred to the web version of the article.)

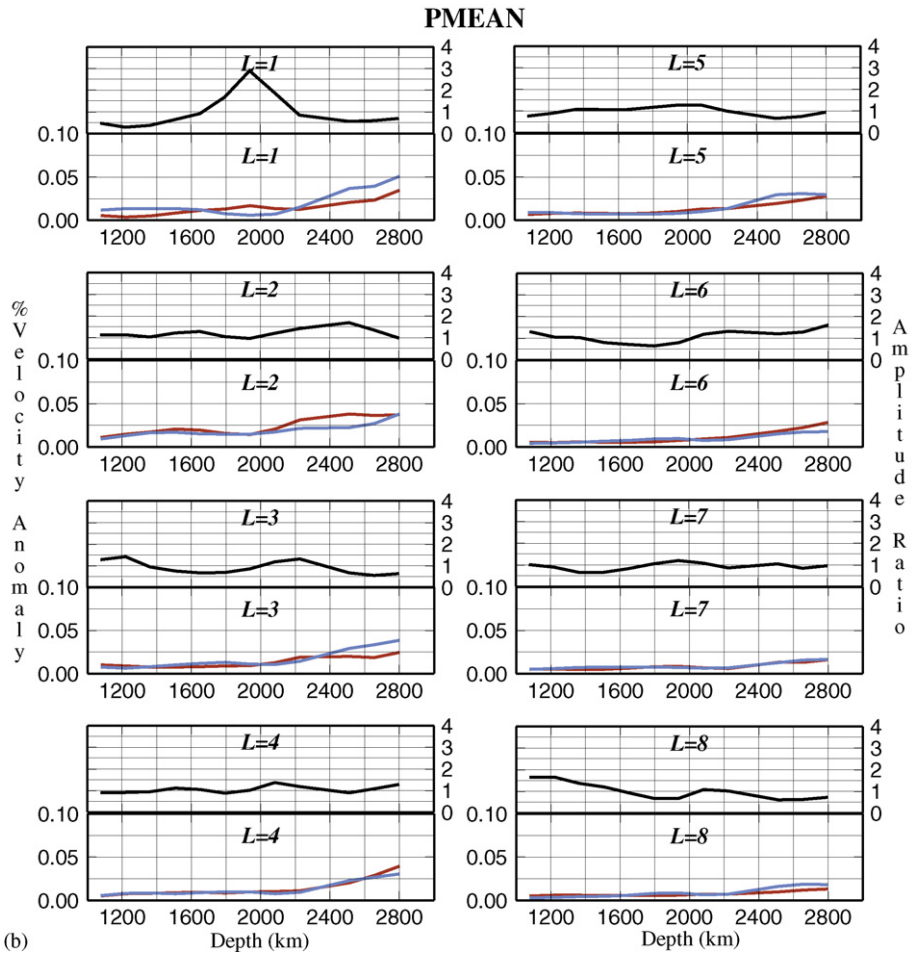

Fig. 4. (*Continued*).

one another. If chemical variations involve local iron enrichment, then they should contribute preferentially to the slow anomalies, in accord with previous studies (Kellogg et al., 1999; van der Hilst and Karason, 1999; Forte and Mitrovica, 2001; Ishii and Tromp, 2004; Trampert et al., 2004). For comparison, the lack of observation of a slab (or thermally cool) signature through the deep mantle is difficult to explain with our current understanding of slab dynamics. Therefore, it is likely that the magnitude and characteristics of slab deformation as the lithosphere traverses from the surface to the core may not be fully represented within current dynamic models, a conclusion in accord with that derived primarily for the transition zone by Becker and Boschi (2002). Dynamic models that incorporate an initial chemically distinct layer near the CMB can result in broad warm features near the CMB that are similar to the broad slow features in tomographic models (Tackley, 1998; Nakagawa and Tackley, 2005; O'Neill et al., 2009), but it is difficult to evaluate the corresponding cool/fast features. The key benefit of our analysis is that it provides a quantitative means to compare both the dominant broad features and narrower features with lower amplitude in tomographic and dynamic models.

Applying our technique to the ratio of fast and slow anomalies of SMEAN, Boschi et al. (2007) also find that the slow anomalies dominate at harmonic degrees less than 14 extending from the CMB to around 1500 km depth and that the fast anomalies have a slightly higher amplitude for harmonic degrees 14–18 extending throughout the lower mantle. We also find the slow anomalies maintain their degree 2 structure throughout much of the lower mantle (Fig. 2g). We do not observe a depth at which higher-order harmonics have larger amplitudes than lower-order harmonics or a depth at which the degree 2 signal diminishes abruptly. Therefore, our analysis does not indicate a depth at which proposed 'plume farms' might spawn smaller plumes (Schubert et al., 2004). If these smaller plumes are below the present tomographic detection threshold, the degree 2 signal would be much smaller for layers above the LLSVP.

We also examine whether similar spatial patterns are observable for a compressional velocity model as for the shear velocity models since compressional models have less amplitude variations within the LLSVP. We found the same pattern of amplitude domination in the slow anomalies at long wavelengths (especially at degree 2, Fig. 4a) and amplitude domination in the fast anomalies at short wavelengths (above degree 13, Fig. 5) in the lower mantle *P* velocity model HMSL-P06 (Houser et al., 2008). This pattern is not observed in PMEAN (Fig. 4b) which is constructed from short-period compressional velocity models. The fast and slow anomalies of SMEAN and PMEAN have very similar amplitudes at the higher harmonic degrees (Fig. 5), thus the ratio of the two is close to one and a dominance of the fast anomalies is not observed in these average models.

The separation spectrum analysis presented here accomplishes two main goals: (1) it provides a technique to perform more detailed comparisons between tomographic and dynamic models than has been done in the past, and (2) it demonstrates that the signal in the fast anomalies is much smaller than predicted by a majority of dynamic models. We have used the most recent mantle shear velocity models to evaluate what tomography can reveal about the relative length-scales of plausible mantle upwellings and downwellings in the bottom 1800 km of the Earth's mantle. The amplitudes in the spherical harmonics for both fast and slow

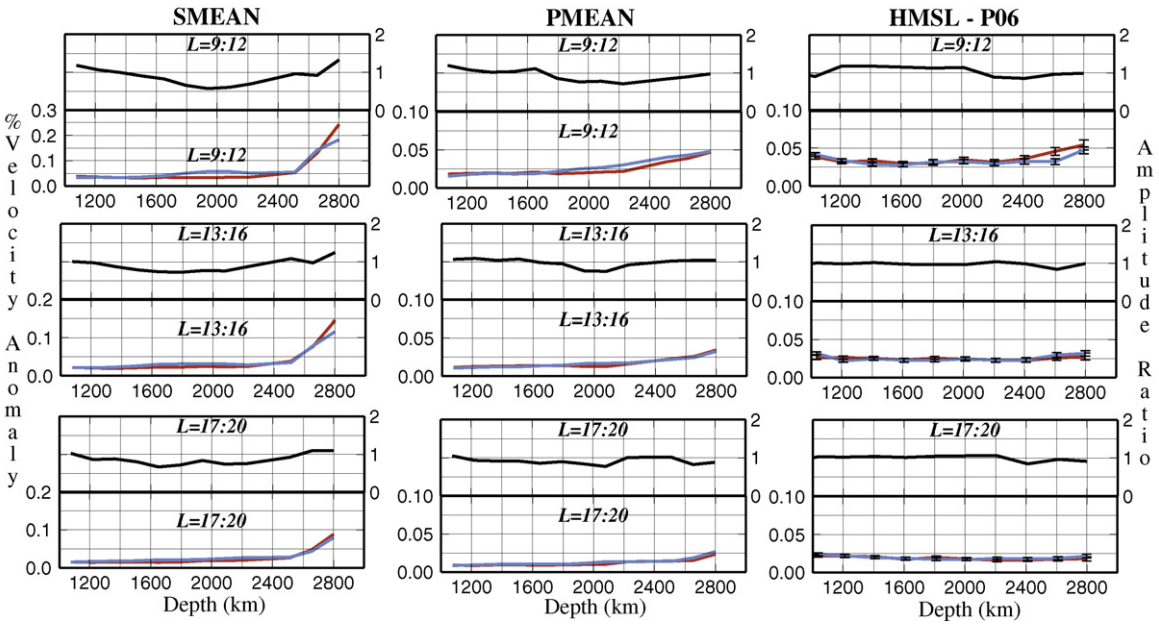

Fig. 5. Amplitude as a function of depth for the summation of spherical harmonic degrees 9–12 (top), 13–16 (middle), and 17–20 (bottom) for the fast anomalies (blue) and slow anomalies (red) for the lower mantle of the compressional velocity model HMSL-P06 (Houser et al., 2008) as well as the averaged models for shear velocity (SMEAN) and compressional velocity (PMEAN) from Becker and Boschi (2002). The black line in the top graph for each harmonic degree is the ratio of amplitudes of the slow and fast anomalies. For HMSL-P06, the amplitude in the fast anomalies overcomes that in the slow anomalies as the harmonic degree increases (wavelength decreases). The ratio of the slow and fast anomaly amplitudes is close to one at all depths at these higher harmonic degrees. (For interpretation of the references to colour in this figure legend, the reader is referred to the web version of the article.)

shear velocity anomalies are dominated by long-wavelength structures. Also, the slow anomalies have higher amplitudes than the fast anomalies at long length-scales, while the fast anomalies have higher amplitudes than the slow anomalies at short length-scales. These observations, when coupled with the lack of a continuous slab signature from the transition zone to the core-mantle boundary, suggest that a simple, first-order picture of the dynamics of a homogeneous mantle is incomplete. The common notion that slabs are continuous features from the surface to the core-mantle boundary and that narrow plumes arise from the core-mantle boundary or from the LLSVP is not consistent with the relative wavelengths of fast and slow velocity anomalies within current tomographic models. Our results are thus consistent with the slow (and possibly the fast) anomalies in the deep mantle being generated by compositional effects, phase changes, and/or extreme lateral variations in viscosity.

Acknowledgement

We thank the University of California Office of the President for providing funding for this work through the University of California Office of the President's Postdoctoral Fellowship Program.

References

Antolik, M., Gu, Y., Ekstrom, G., Dziewonski, A., 2003. J362D28: a new joint model of compressional and shear velocity in the Earth's mantle. Geophys. J. Int. 153, 443–466.

Bassin, G., Laske, G., Masters, G., 2000. The current limits of resolution for surface wave tomography in North America. Eos. Trans. Am. Geophys. U. 81, 897.

Becker, T.W., Boschi, L., 2002. A comparison of tomographic and geodynamic mantle models. Geochem. Geophys. Geosys. 3, doi:10.1029/2001GC0001682.

Boschi, L., Becker, T.W., Steinberger, B., 2007. Mantle plumes: dynamic models and seismic images. Geochem. Geophys. Geosys. 8, Q10006, doi:10.1029/2007GC001733.

Bunge, H.-P., 2005. Low plume excess temperature and high core heat flux inferred from non-adiabatic geotherms in internally heated mantle circulation models. Phys. Earth Plant. Inter. 153, 3–10.

Bunge, H.-P., Richards, M.A., Baumgardner, J.R., 1996. The effect of depth dependent viscosity on the planform of mantle convection. Nature 379, 436–438.

Bunge, H.-P., Richards, M.A., Baumgardner, J.R., 1997. A sensitivity study of 3-D spherical mantle convection at 10^8 Rayleigh number: effects of depth dependent viscosity, heating mode and an endothermic phase change. J. Geophys. Res. 102, 11991–12007.

Courtillot, V., Davaille, A., Besse, J., Stock, J., 2003. Three distinct types of hotspots in the Earth's mantle. Earth Planet. Sci. Lett. 205, 295–308.

Davaille, A., Le Bars, M., Carbonne, C., 2003. Thermal convection in a heterogeneous mantle. C. R. Geosci. 335, 141–156.

Deschamps, F., Tackley, P.J., 2008. Searching for models of thermo-chemical convection that explain probabilistic tomography. I. Principles and influence of rheological parameters. Phys. Earth Planet. Inter. 171, 357–373.

Dziewonski, A., Hager, B., O'Connell, R.J., 1977. Large-scale heterogeneities in the lower mantle. J. Geophys. Res. 82, 239–255.

Edmonds, A.R., 1960. Angular Momentum in Quantum Mechanics. Princeton University Press, Princeton, NJ.

Forte, A.M., Mitrovica, J.X., 2001. High viscosity deep mantle flow and thermochemical Structure inferred from seismic and geodynamic data. Nature 410, 1049–1056.

Gu, Y.J., Dziewonski, A.M., Su, W.-J., Ekström, G., 2001. Models of the mantle shear velocity and discontinuities in the pattern of lateral heterogeneities. J. Geophys. Res. 106, 11169–11199.

Hager, B., Clayton, R., Richards, M., Comer, R., Dziewonski, A., 1985. Lower mantle heterogeneity, dynamic topography and the geoid. Nature 313, 541–545.

Hernlund, J.W., Houser, C., 2008. On the statistical distribution of seismic velocities in the Earth's deep mantle. Earth. Planet. Sci. Lett. 265, 423–437, doi:10.1016/j.epsl.2007.10.042.

Houser, C., Masters, G., Shearer, P., Laske, G., 2008. Shear and compressional velocity models of the mantle from cluster analysis of long-period waveforms. Geophys. J. Int. 174, 195–212.

Ishii, M., Tromp, J., 2004. Constraining large-scale mantle heterogeneity using mantle and inner-core sensitive normal modes. Phys. Earth Planet. Inter. 146, 113–124.

Jellinek, A.M., Manga, M., 2004. Links between long-lived hotspots, mantle plumes, D" and plate tectonics. Rev. Geophys. 42 (3), RG3002, doi:10.1029/2003RG000144.

Kellogg, L.H., Hager, B.H., van der Hilst, R., 1999. Compositional stratification in the deep mantle. Science 283, 1881–1884.

McNamara, A., Zhong, S., 2005. Thermochemical structures beneath Africa and the Pacific Ocean. Nature 437, 1136–1139.

Megnin, C., Bunge, H.-P., Romanowicz, B., Richards, M.A., 1997. Imaging 3-D spherical convection models: what can seismic tomography tell us about mantle dynamics? Geophys. Res. Lett. 11, 1299–1302.

Megnin, C., Romanowicz, B., 2000. The three-dimensional shear velocity structure of the mantle from the inversion of body, surface, and higher-mode waveforms. Geophys. J. Int. 143, 709–728.

Montelli, R., Nolet, G., Dahlen, F.A., Masters, G., 2006. A catalogue of deep mantle plumes: new results from finite frequency tomography. Geochem. Geophys. Geosys. 7, doi:10.1029/2006GC001248.

Nakagawa, T., Tackley, P.J., 2004. Thermo-chemical structure in the mantle arising from a three-component convective system and implications for geochemistry. Phys. Earth Planet. Inter. 146, 125–138.
Nakagawa, T., Tackley, P.J., 2005. Deep mantle heat flow and thermal evolution of the Earth's core in thermochemical multiphase models of mantle convection. Geochem. Geophys. Geosyst. 6, Q08003, doi:10.1029/2005GC000967.
O'Neill, C., Lenardic, A., Jellinek, A.M., Moresi, L., 2009. Influence of supercontinents on deep mantle flow. Gondwana Research 15, 276–287.
Ritsema, J., van Heijst, H.J., 2000. Seismic imaging of structural heterogeneity in Earth's mantle: evidence for large-scale mantle flow. Sci. Prog. 83, 243–259.
Schubert, G., Masters, G., Olson, P., Tackley, P., 2004. Superplumes or plume clusters? Phys. Earth Planet. Inter. 146, 147–162.
Simmons, N.A., Forte, A.M., Grand, S.P., 2006. Constraining mantle flow with seismic and geodynamic data: a joint approach. Earth Planet. Sci. Lett. 246, 109–124.
Sleep, N.H., 1990. Hotspots and mantle plumes: some phenomenology. J. Geophys. Res. 95, 6715–6736.
Su, W.-J., Dziewonski, A.M., 1991. Predominance of long-wavelength heterogeneity in the mantle. Nature 352, 121–126.
Tackley, P.J., Stevenson, D.J., Glatzmaier, G.A., Schubert, G., 1993. Effects of an endothermic phase transition at 670 km depth in a spherical model of convection in the Earth's mantle. Nature 361, 699–704.
Tackley, P.J., 1998. Three-dimensional simulations of mantle convection with a thermochemical CMB boundary layer: D"? In: Gurnis, et al. (Eds.), The Core-Mantle Boundary Region. American Geophysical Union, Geophysics Monograph, pp. 231–253.
Tan, E., Gurnis, M., 2002. Slabs in the lower mantle and their modulation of plume formation. Geochem. Geophys. Geosys. 3, doi:10.1029/2001GC000238.
Thorne, M., Garnero, E., Grand, S., 2004. Geographic correlation between hot spots and deep mantle lateral shear-wave velocity gradients. Phys. Earth Planet. Inter. 146, 47–63.
Trampert, J., Deschamps, F., Resovsky, J., Yuen, D., 2004. Probabilistic tomography maps chemical heterogeneities throughout the lower mantle. Science 306, 853–856.
van der Hilst, R., Widiyanatoro, S., Engdahl, E.R., 1997. Evidence for deep mantle circulation from global tomography. Nature 388, 578–584.
van der Hilst, R.D., Karason, H., 1999. Compositional heterogeneity in the bottom 1000 kilometers of the Earth's mantle: toward a hybrid convection model. Science 283, 1885–1888.
Woodward, R., Masters, G., 1991a. Global upper mantle structure from long-period differential travel times. J. Geophys. Res. 96, 6351–6377.
Woodward, R., Masters, G., 1991b. Lower mantle structure from *ScS-S* differential travel times. Nature 352, 231–233.
Woodward, R., Dziewonski, A., Peltier, W.R., 1994. Comparisons of seismic heterogeneity models and convective flow calculations. Geophys. Res. Lett. 21, 325–328.
Yanagisawa, T., Hamano, Y., 1999. "Skewness" of S-wave velocity in the mantle. Geophys. Res. Lett. 26, 791–794.
Zhang, S.X., Yuen, D., 1996. Various influences on plumes and dynamics in time-dependent, compressible mantle convection in 3D spherical shell. Phys. Earth Planet. Inter. 94, 241–267.
Zhong, S., Gurnis, M., 1997. Dynamic interaction between tectonic plates, subducting slabs, and the mantle. Earth Interactions 3, 1–8.